Brook D. Ferney
Steven L. Folkman
Mechanical and Aerospace Engineering Department
Utah State University
Logan, UT 84322-4130

Force-State Characterization of Struts Using Pinned Joints

As part of a research effort to study the microgravity dynamics of a truss with pinned joints, a single strut with a single clevis-tang pinned joint was characterized. Experimental data was collected using a force-state mapping technique. The strut was subjected to axial dynamic loads and the response of the strut was measured. The force-state map aids visualization of the strut dynamics. Finite element modeling of the response was explored. An example is presented that uses a method of manual determination of the finite element model parameters. The finite element model results correspond well with the measured strut response. © *1997 John Wiley & Sons, Inc.*

INTRODUCTION

Deployable space structures typically incorporate multiple revolute (e.g., pinned) joints. If the joint design allows a small amount of "slop" or deadband, the dynamic behavior of the structure can be dramatically altered. The deadband and friction characteristics in this type of joint can introduce nonlinearities into the joint behavior. Nonlinear response in these joints is difficult to predict and can therefore limit the use of such a truss. Folkman and colleagues (1995) reported tests of a truss using a few pinned joints and compared the results with the same truss but with the joints tightly clamped together. When preloads were small, the truss using pinned joints had significantly more damping and exhibited nonlinear behavior. They reported that when large preloads were applied across pinned joints in the truss, the damping was reduced and the dynamic behavior was very similar to the truss using only tightly clamped joints. Several authors discussed cases where preloaded joints acted nonlinearly (Chattopadhyay, 1993; Den Hartog and Mikina, 1932). Unfortunately, dynamic behavior due to the joints is very dependent on many variables such as the joint design and the condition of joint interfaces. Predicting the dynamic behavior is difficult at best. Measured data from design prototypes is often required.

Large-scale testing, if practiced at all, usually occurs after most of the structural design has been fixed in detailed design drawings. Design changes dictated by the test data this late in the design would be costly. In many cases such testing may not be feasible due to the structure's size and the influence of gravity. However, early testing of structural elements is possible and can provide valuable information to support the design process. One approach to the testing of a large truss could be to test individual struts to characterize these elements for use in overall system models. The present article presents one method for experimentally gathering and evaluating the data for an individual strut and characterizing the response by finite element modeling techniques. An implicit assumption here is that the behavior in these component tests simulates the behavior of the component in the complete structure. This assumption will be validated if and only if the assembled structure's behavior is successfully predicted by a finite element model of the assembled structure com-

Received August 17, 1995; Accepted September 18, 1996.
Shock and Vibration, Vol. 4, No. 2, pp. 103–113 (1997)

CCC 1070-9622/97/020103-11

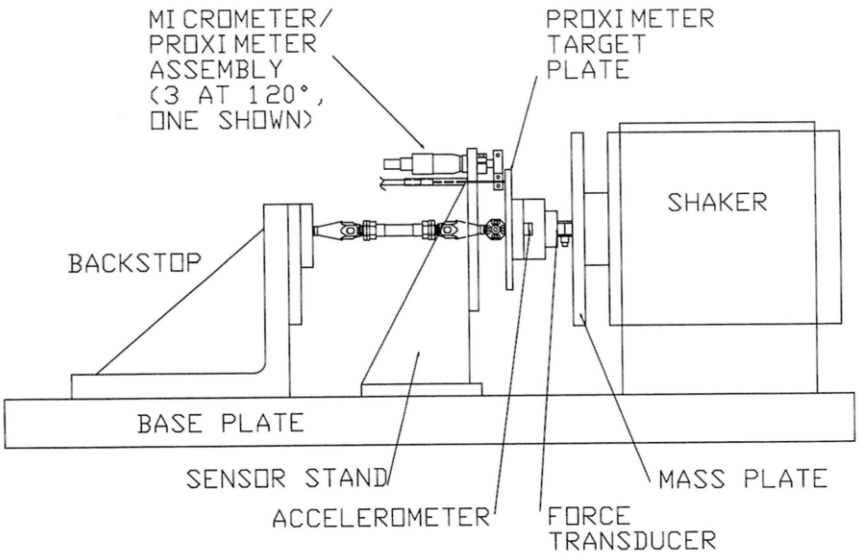

FIGURE 1 Illustration of the force-state map test setup.

posed of the individual strut models. Dutson and Folkman (1996) reported that this approach was successful in simulating many important aspects of the behavior of a truss.

The experimental method used is the force-state mapping (FSM) approach described by Crawley and Aubert (1986). The method involves the determination of the restoring force function, $f(x, \dot{x})$, based upon the surface formed by recording the net force, $F - m\ddot{x}$, over a range of the

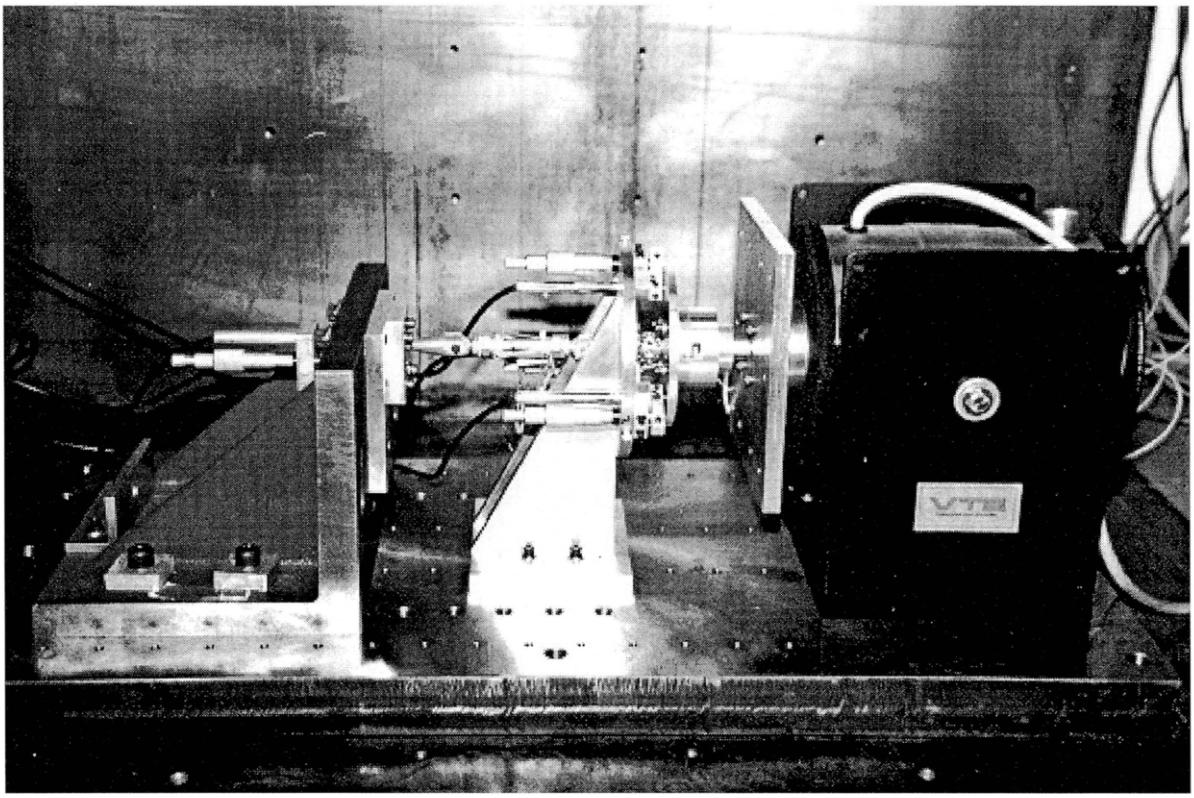

FIGURE 2 Photograph of the force-state map test setup.

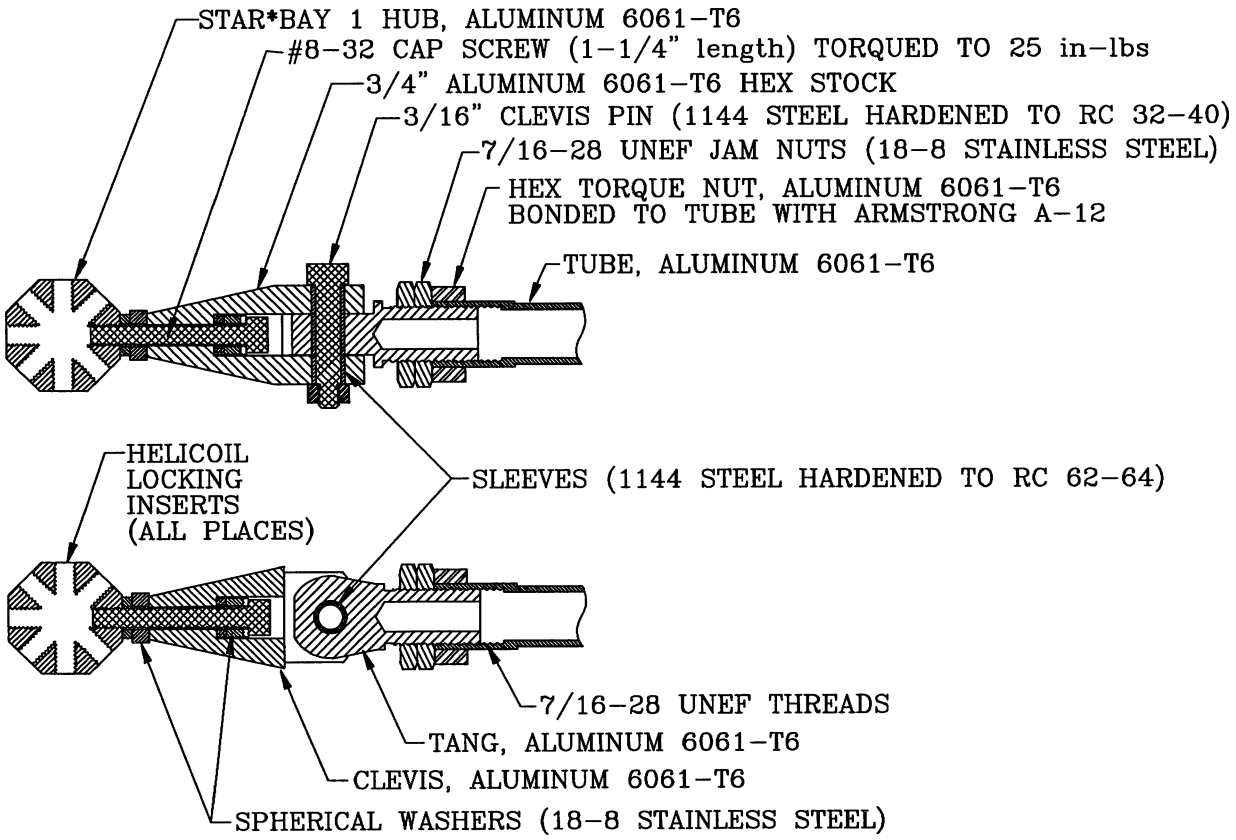

FIGURE 3 Illustration of the clevis/tang joint design.

state variables, displacement and velocity. These are related in Eq. (1).

$$f(x, \dot{x}) = F - m\ddot{x}. \tag{1}$$

In this equation, F is the applied force and is of the form $F = F_{\max} \sin(\omega t)$ for this research. The $m\ddot{x}$ term represents the inertial resistance of the system.

Masri and Caughey (1979) used Chebyshev polynomials to nonparametrically approximate the restoring force function. Crawley and Aubert (1986) designed experiments to show the ability of FSM to measure nonlinear behavior. They presented a typical map for cushiond impact. Their results showed the potential of the technique and the possibility of identifying combined effects in a single map. Crawley and O'Donnell (1987) further refined the test setup and validated it with several test articles. They also studied a laterally excited pinned joint with and without a locking sleeve and were able to identify friction nonlinearities that were not of the simple Coulomb type. Masters and Crawley (1994) extended their research on FSM to include multiple degrees of freedom (MDOF). Masters et al. (1996) continued the MDOF component characterization using FS maps. The components were combined into a global model that was rather successful at predicting the nonlinear response of their truss.

A study of a NASA-developed clevis-tang joint that incorporated preloaded bearings was conducted by Bullock and Peterson (1994). The joint exhibited linear response down to the micron level of motion. They concluded that no simple single DOF FSM model could accurately represent the submicron nonlinearities of the joint. The behavior of the internal joint components is not negligible and appears to couple the joint's six rigid body DOFs. Therefore, the observed nonlinear behavior is attributable to some combination of DOF coupling and the effects of unmeasured states on the FSM.

No general model is available describing energy losses in joints. However, analytical and computer models that attempt to include friction and impacting of a structure containing a single joint are available (see Dubowsky, 1974; Dubowsky and Freudenstein, 1971; Ferri, 1988). Ferri (1988)

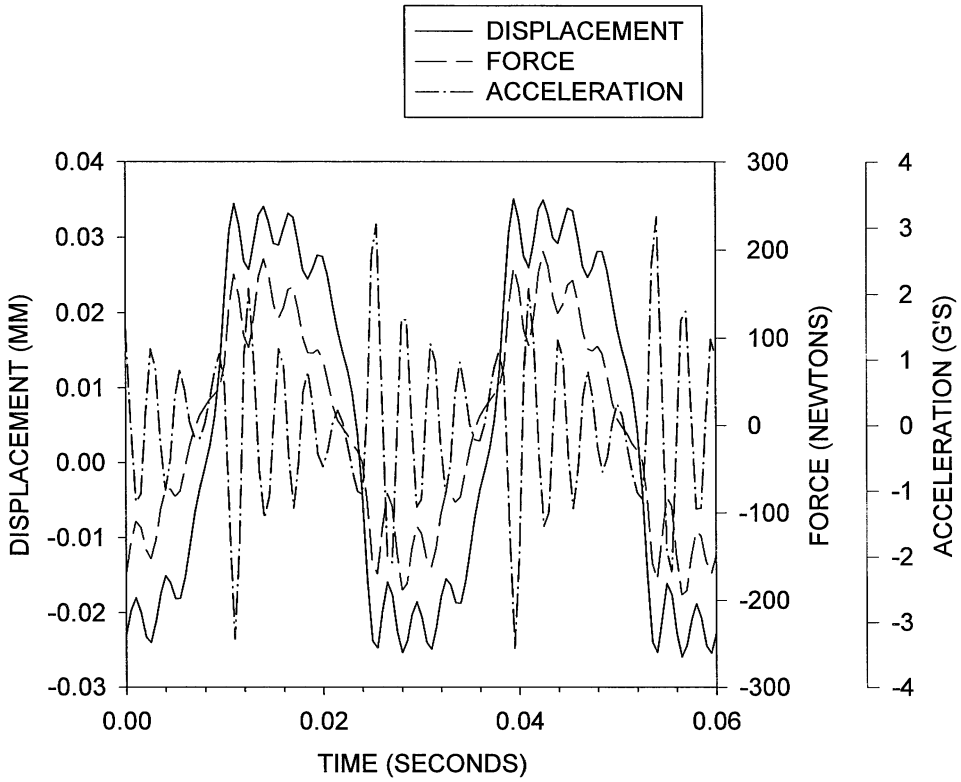

FIGURE 4 Illustration of the measured time history for a 35-Hz test.

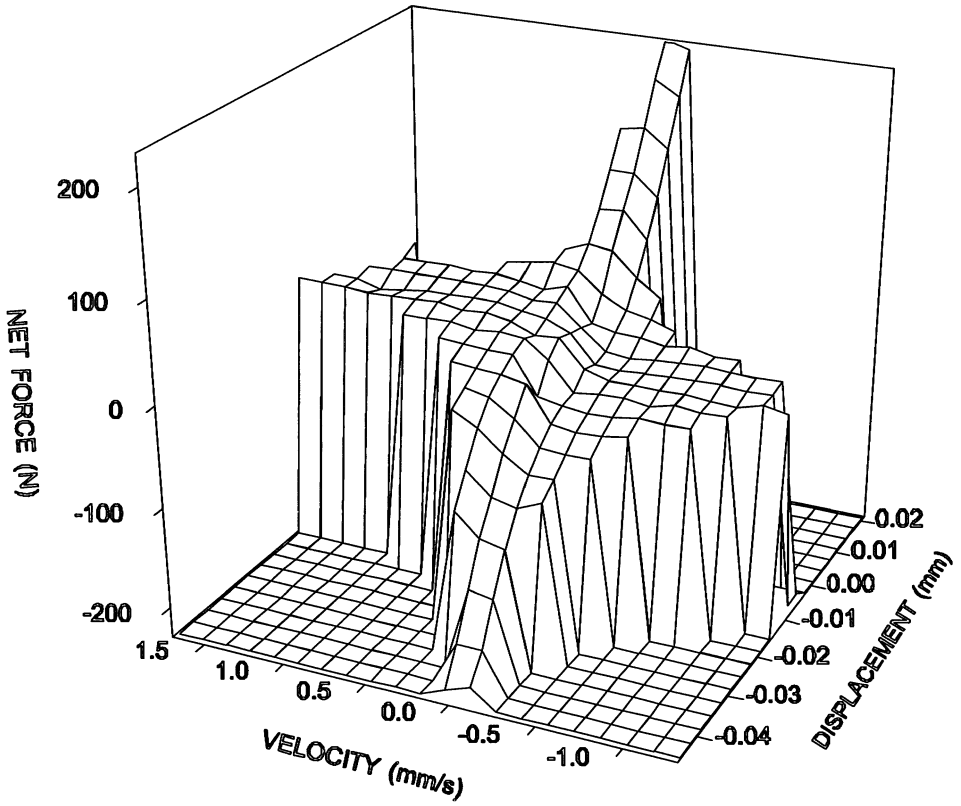

FIGURE 5 Force-state map of measured data for the short strut with a 4.729 mm (0.1862 in.) pin and 1-Hz forcing frequency.

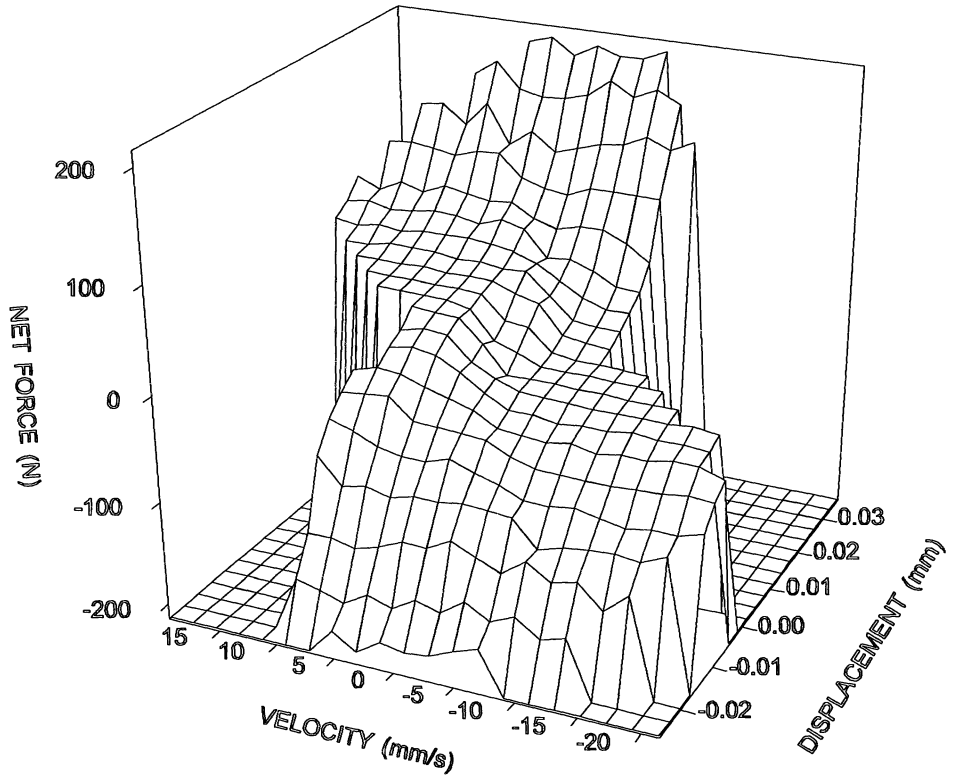

FIGURE 6 Force-state map of measured data for the short strut with a 4.729 mm (0.1862 in.) pin and 35-Hz forcing frequency.

showed computer simulations of the behavior of a single joint indicating that nonlinear sources of damping, such as friction and impacting, appear to be predominately viscous in nature. The models in the above references are not directly applicable to truss structures with multiple joints, although they could provide damping estimates of individual components.

Using FSM testing to assist in developing a finite element model of a truss structure using pinned joints was proposed by Belvin (1987). He developed nonlinear finite element models of a truss based on strut characterization testing. Belvin's work focused on very large space structures and was limited to low frequencies. He was able to neglect the influence of impacting in the joints because the frequencies were very low. This article is similar to Belvin's work but focuses on higher frequencies where impacting is significant.

This research is different than previously reported studies using the FSM technique to characterize strut behavior. The strut is not preloaded and when axial loads are applied to the strut, the deadband region of the joint is traversed. The joint experiences deadband, friction forces, and "hard" impacts. A hard impact is defined here as one where a small shock force is generated and the system can rebound. The research objective is to obtain FSM data and investigate how it can be used to model a single strut.

EXPERIMENTAL SETUP

Figure 1 illustrates the test setup. The test bed was designed to accomodate struts of various lengths and to test in either a horizontal or vertical orientation, although the horizontal orientation was used. A 2-in. thick steel plate mounted to a 1-in. thick steel plate, which was secured to the floor, was used. A cast steel backstop was used as a semirigid reference to which a test piece was mounted. A 222 N (50 lb) electrodynamic vibrator applied a force to one end of the strut. A force transducer and an accelerometer were mounted axially at the point of load application. Three fiber optic displacement sensors were placed at 120° intervals around the strut. The high output range of these sensors is approximately ±0.051 mm (±0.002 in.). Averaging the output of the three produced the

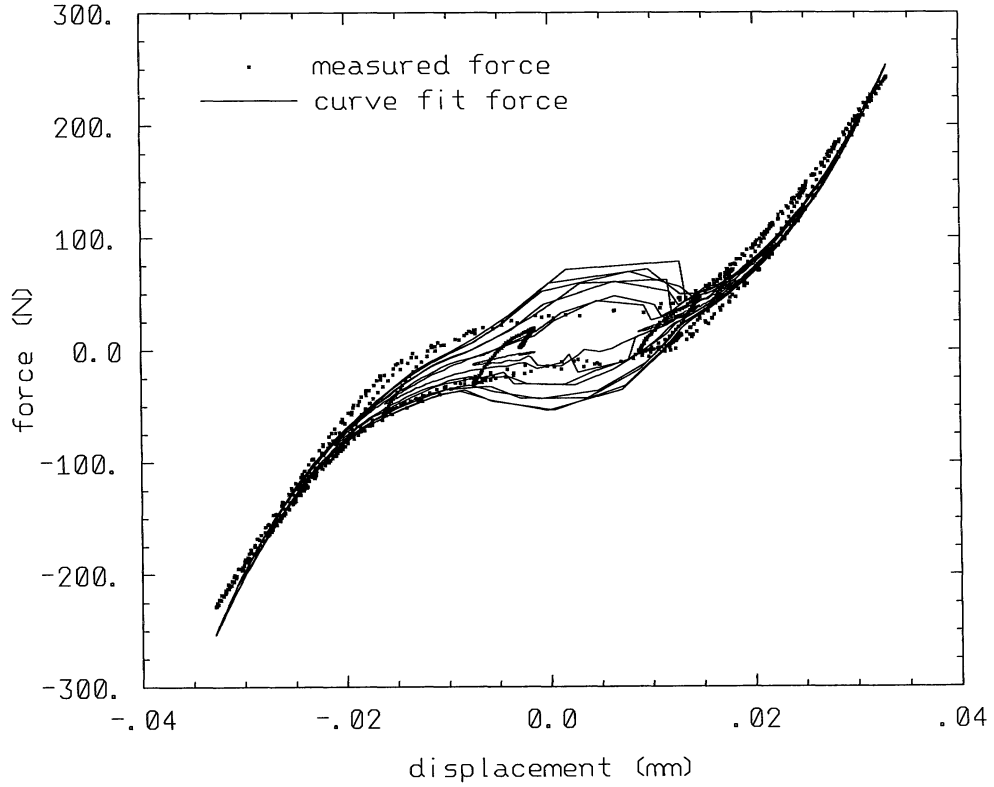

FIGURE 7 Plot showing the data for the short strut with a 4.729 mm (0.1862 in.) pin and 1-Hz forcing frequency compared to the curve fit given by Eq. (2).

axial displacement without bending effects. Figure 2 is a photograph of the test setup.

The velocity is obtained by differentiating the displacement data using a three-point central difference formula. This was chosen over integration of the accelerometer data because the signal from the accelerometer contained more noise than that from the displacement sensors. Velocities obtained by differentiating the displacement data were smoother than those obtained be integrating the acceleration data. The second derivative of the displacement data was also compared to the accelerometer data and was found to correspond nicely except that the second derivative of the displacement signal contained more noise than the accelerometer data. The increase in noise was due to the numerical differentiation process.

The accuracy of the test bed was verified by testing aluminum tubing with known stiffness and low damping characteristics. Initial tests demonstrated that small displacements could occur in the backstop. To compensate for this movement, a fourth displacement sensor was added to measure the motion of the fixed end. One displacement sensor is adequate because it can be mounted axially with the strut. The axial elongation of the strut was found as the average of the front end displacements minus the back end displacement. This elongation was then differentiated to find the velocity. Measured and predicted stiffness data for the tubing indicated reasonable agreement for stiffness values in the range of the struts to be tested.

The strut has two types of joints. On one end the joint has a press fit pin and behaves linearly. The other end has a clearance fit pin as illustrated in Fig. 3. Tang and clevis holes are press fit with hardened steel inserts. The pin is a shoulder bolt. The hardness of the pin and the sleeves is intended to reduce wear and therefore reduce dimensional changes affecting performance. This hard interface encourages impacting and rebounding as the pin and sleeve make contact. The deadband in the pinned joint is adjusted by using different diameter pins.

Testing was done with two tube lengths, three pin diameters, and three forcing frequencies. The two tube lengths allowed testing of a short strut with an overall length of 203.2 mm (8.0 in.) and a long strut with an overall length of 400 mm (11.3

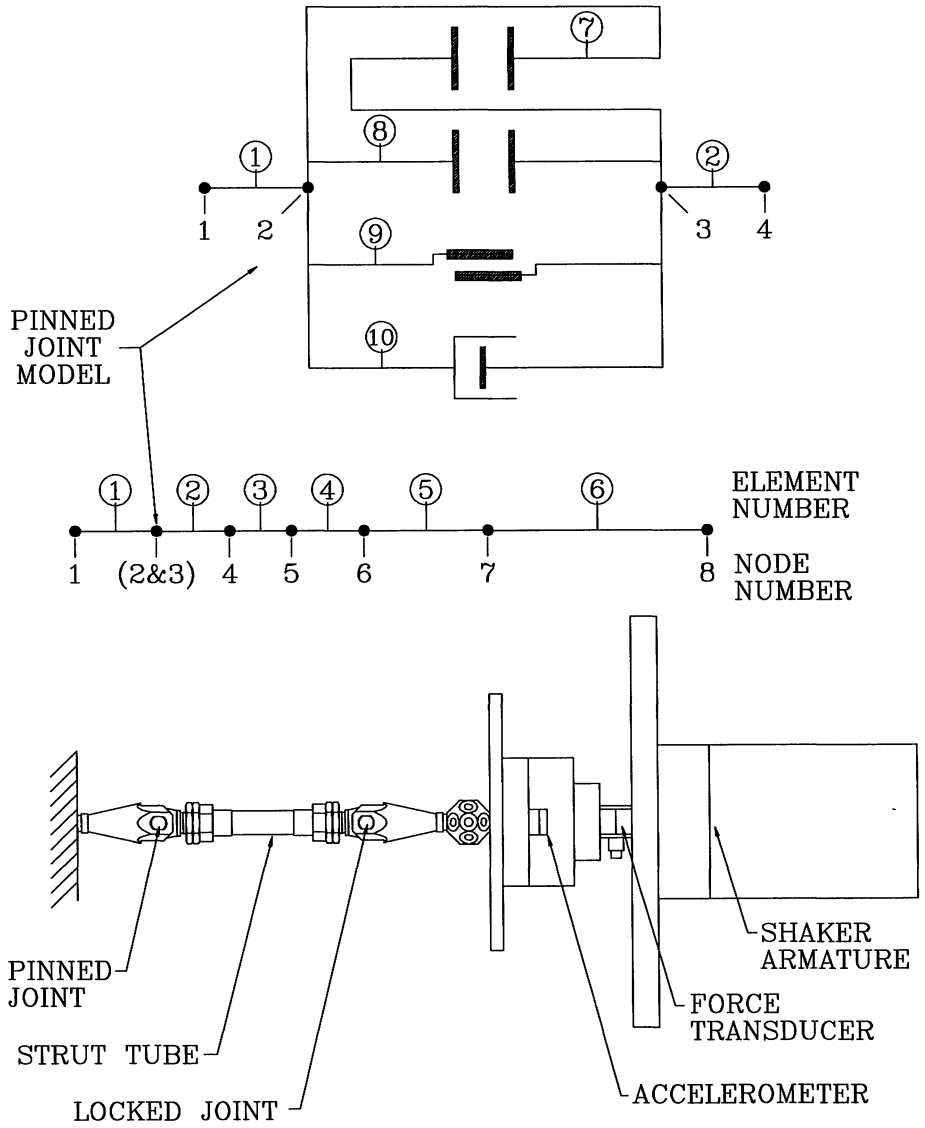

FIGURE 8 Illustration of the strut in the test bed and the corresponding finite element model.

in.). The three pin diameters were 4.729 mm (0.1862 in.), 4.735 mm (0.1864 in.), and 4.740 mm (0.1866 in.). The hole diameter was 4.752 mm (0.1871 in.). Forcing frequencies were 1, 35, and 100 Hz, corresponding to quasistatic condition and two vibration modes of a truss that used the struts being tested.

To fill in the restoring force surface, a range of testing amplitudes was recorded. This was done using an amplitude modulated forcing function. One period of the modulating signal was recorded. Thus, the state space was traversed twice. Data rates up to 8000 samples per second were tested to ensure that all of the dynamic characteristics were recorded. Due to memory limitations the tests were recorded at 200 samples per second for the 1-Hz tests, 2000 samples per second for the 35-Hz tests, and 4000 samples per second for the 100-Hz tests.

RESULTS

Initially it seemed that the results in the time domain included too many high frequency vibrations and rebounds to form a single surface. Example raw data in the time domain can be seen in Fig. 4. However, for a given test frequency, the restoring

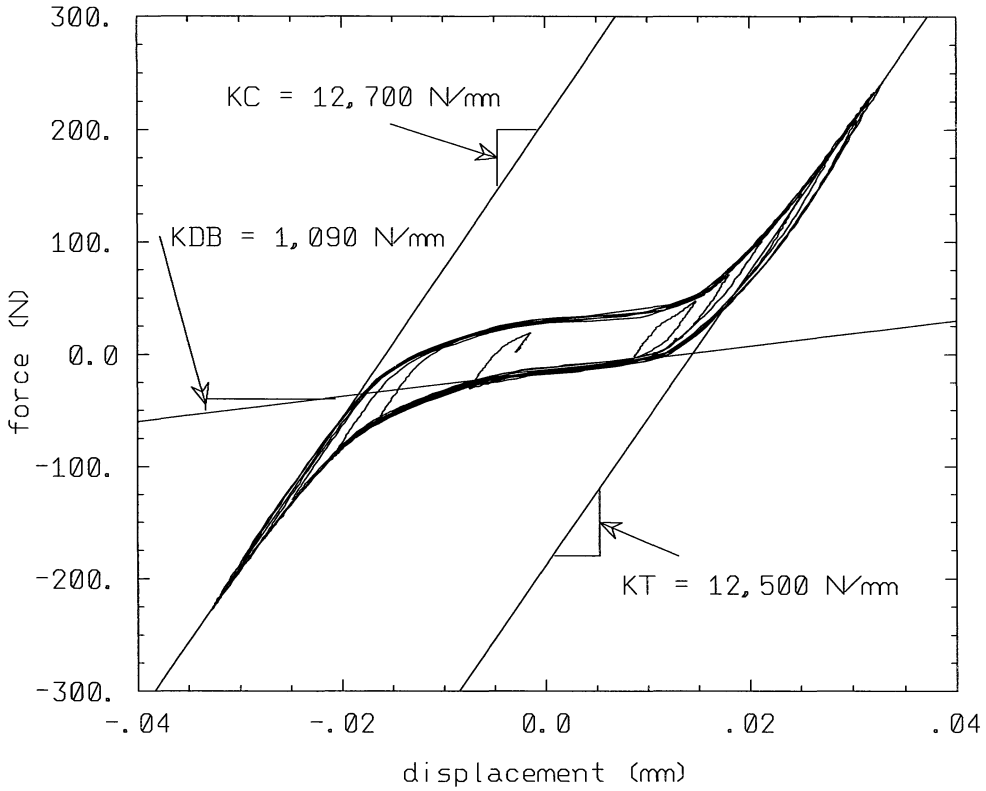

FIGURE 9 Illustration of the determination of stiffness from quasistatic test data for the finite element model.

force is a single surface in the force-state domain, even when hard impacts occur.

Figures 5 and 6 show the FSM surface formed by the tests on a short strut with a 4.729 mm (0.1862 in.) pin at 1 and 35 Hz forcing frequencies, respectively. These figures were constructed by laying a grid over the state space and averaging the force data around each grid point to get the value of that grid point. It was necessary to adjust the grid size such that it was small enough so that all of the nonlinearities were visible, but large enough to not have holes at points in the state space where no data had been taken. Visually it is possible to identify several nonlinear effects, which is the value of the FSM. The deadband is evident in the displacement direction. Due to the deadband, the force-displacement response is very cubic in nature. In the deadband region, the velocity data makes a step at the origin. This is easily observed in Fig. 5 and is indicative of Coulomb friction forces being present in the joint. Figure 5 is described as a quasistatic test because the velocities are low. The effect of impacting should be minimal in Fig. 5 and friction in the joint should be the primary damping mechanism. Outside of the deadband region, the force-velocity response appears to be flat, but it actually has a small linear slope in Figs. 5 and 6. This could be modeled as linear viscous damping. Also note that the FSM surfaces in Figs. 5 and 6 are different. That is, the FSM surface obtained is dependent on the forcing function frequency.

To use this surface as an aid in model development, a restoring function could be assumed and fit to the surface. Higher order functions have been used to simulate FSM behavior (see Belvin, 1987; Masri and Caughey, 1979). The objective of this research is to simulate the behavior of the strut using a commercial finite element program. Thus, it is desirable to fit a relatively simple function to the surface, which is consistent with the capabilities of the finite element program. The stiffness in the simple model could be determined using two different sets of terms. The first would be a linear and a cubic stiffness term. This would fit the data best because it appears to be very cubic. The second is a piecewise linear fit. This fit would include linear terms representing the stiffness in the tension, compression, and deadband zones. These linear terms are easiest to include in a finite element

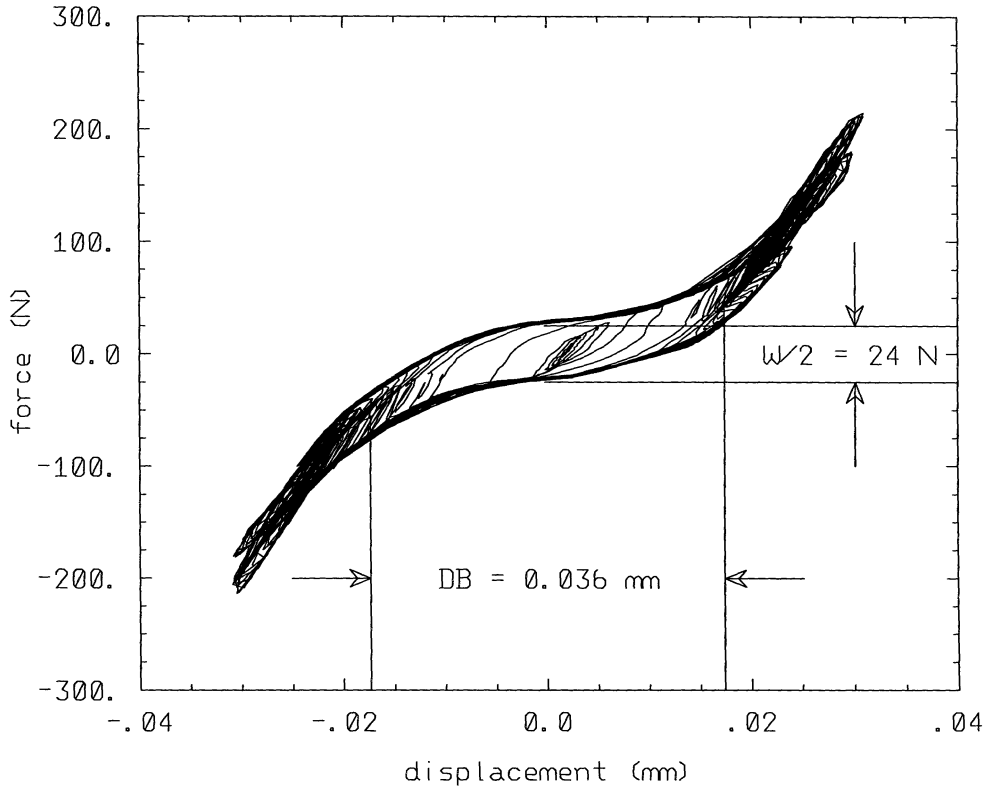

FIGURE 10 Illustration of the determination of deadband parameters from dynamic test data for the finite element model.

model. The damping terms could be linear viscous damping and/or Coulomb friction damping.

Equation (2) represents a typical restoring function that includes linear and cubic stiffness terms along with linear viscous damping and Coulomb friction terms.

$$f(x, \dot{x}) = Kx + K_3x^3 + B\dot{x} + N\,\text{sign}(\dot{x}). \quad (2)$$

Figure 7 illustrates the least squares fit of Eq. (2) to the measured data illustrated in Fig. 5. The measured data in Fig. 7 is for the short strut with a 4.729 mm (0.1862 in.) pin and a 1-Hz forcing frequency. It is very difficult to visually compare two FSM surfaces. To simplify the comparison, Fig. 7 illustrates a 2-dimensional view of the FSM data. Thus, a number of cycles over a range of amplitudes are shown in Fig. 7. The multiple curves represent different amplitudes of the forcing function. The fit fails to represent the force surface without applying different damping terms in different regions. For example, the viscous term could be applied only in the tension and compression zones and the Coulomb friction term could be applied only in the deadband zone. This motivated moving to a piecewise linear approach.

A finite element model of the strut in the test bed was developed and analyzed using MSC/NASTRAN. A primary objective was to find a simple method of simulating the deadband and impacting that would occur. MSC/NASTRAN has a gap element that can be used to simulate contact between bodies. When contact occurs in a gap element, a high stiffness is applied between the bodies in the direction normal to the contact plane and friction forces can be transmitted in directions perpendicular to the contact plane. Based upon the possible nonlinearities in the strut dynamics illustrated in Figs. 5 and 6, a simple finite element model of the strut in the test bed was constructed as shown in Fig. 8. This figure includes an illustration of the corresponding strut in the test bed. Elements numbered 1–6 are beam elements modeling the strut and shaker. Elements 7 and 8 are gap elements that allow deadband during the load cycles. Element 9 is a gap element that provides constant friction forces as the joint traverses the deadband region. Element 10 is a viscous damping

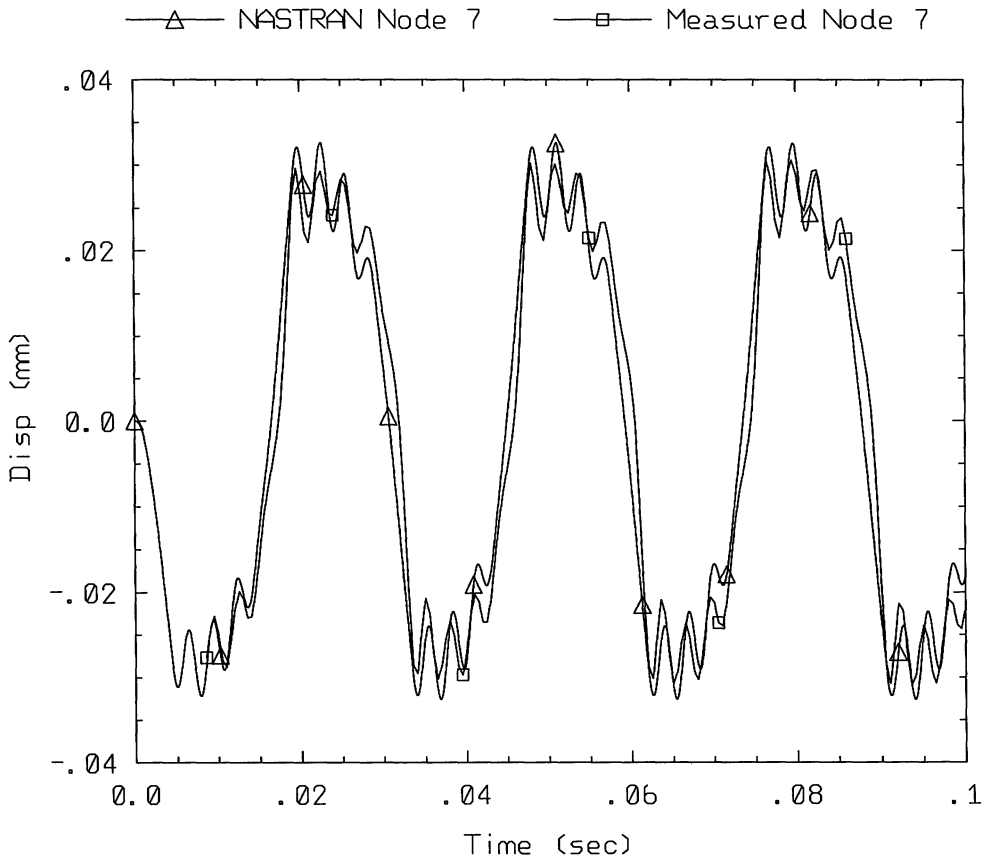

FIGURE 11 Plot showing the comparison between the finite element model run on MSC/NASTRAN and the experimental data for the short strut with a 4.729 mm (0.1862 in.) pin and 35-Hz forcing frequency.

element inside the gap. The small viscous behavior outside the gap was not included in the model. The measured masses were lumped to their respective nodes. The finite element model requires the input of several parameters that can be approximated from the measured data.

First, each beam element must be assigned a stiffness that is a static characteristic. Figure 9 shows the quasistatic FSM data (the same data used to generate the surface in Fig. 5) and the average of the tension and compression stiffness, 12,600 N/mm, which is the overall struct stiffness. The stiffness of the strut tube (element 3) is known from physical dimensions. The remaining elements were adjusted in stiffness such that the combined stiffness equaled the measured overall stiffness. The joint model must be assigned a stiffness for when the gap is open (1090 N/mm from Fig. 9) and a very large stiffness when the gap is closed.

Next, from the FSM data from tests with a 35-Hz forcing frequency, the characteristics of the gap are determined. The width of the deadband is determined from Fig. 10 to be 0.036 mm and is used to set the gap distance in elements 7 and 8 in Fig. 8. Three damping type parameters exist in the model. The friction surface (element 9 in Fig. 8) produces a constant Coulomb type force as the joint traverses the deadband region. The value for this force, 24 N, is found as half of the loop width in Fig. 10. The damping coefficient for element 10 in Fig. 8 was set at 7 N/mm after running the model and refining it to fit better. Each beam element also has material damping. This loss factor was set to 0.008, which is typical for aluminum at low strains.

These parameters were implemented in a MSC/NASTRAN model excited at 35 Hz with an amplitude of 156 N (35 lb). The result is best evaluated by graphical comparison of the displacement–time history for the model and the experimental data. Figure 11 shows this comparison. The results compare very well and indicate that this simple strut

model adequately accounts for the nonlinearities. The next step in model development would be to adjust the parameters from their nominal values until an even better correlation exists. This would result in a very accurate characterization of the behavior of a strut with a pinned joint in a test bed.

CONCLUDING REMARKS

An FSM technique was used to successfully obtain a base of experimental information regarding the axial behavior of struts with pinned joints. This data is useful for the development of finite elements models of struts in a test bed. At this time it is assumed that the boundary conditions in the test bed are similar to those in the truss. For surface fits with simple terms, the fit is deemed not useful unless it can apply different terms in different zones. A better approach was shown to be the determination of nominal parameters from the data with subsequent adjustment until the finite element model and data match on displacement–time history plots. Future work will involve combining the strut model into a truss model.

The funding of this research by NASA (Contract NAS1-19418) and a Vice President's Research Fellowship from Utah State University is gratefully acknowledged.

REFERENCES

Belvin, W. K., 1987, "Modeling of Joints for the Dynamic Analysis of Truss Structures," NASA Technical Paper 2661, NASA, Washington, DC.

Bullock, S. J., and Peterson, L. D., 1994, "Identification of Nonlinear Micron-Level Mechanics for a Precision Deployable Joint," in *Proceedings of the 35th AIAA/ASME/ASCE/AHS/ASC Structures, Structural Dynamics and Materials Conference,* Hilton Head, pp. 331–338.

Chattopadhyay, S., 1993, "Dynamic Response of Preloaded Joints," *Journal of Sound and Vibration*, Vol. 163, pp. 527–534.

Crawley, E. F., and Aubert, A. C., 1986, "Identification of Nonlinear Structural Elements by Force-State Mapping," *AIAA Journal*, Vol. 24, pp. 155–162.

Crawley, E. F., and O'Donnell, K. J., 1987, "Force-State Mapping Identification of Nonlinear Joints," *AIAA Journal*, Vol. 25, pp. 1003–1010.

Den Hartog, J. P., and Mikina, S. J., 1932, "Forced Vibrations with Non-Linear Spring Constants," *Transactions of the ASME*, Vol. 54, pp. 157–164.

Dubowsky, S., 1974, "On Predicting the Dynamic Effects of Clearances in Planar Mechanisms," *ASME Journal of Engineering for Industry*, Vol. 96, pp. 317–323.

Dubowsky, S., and Freudenstein, F., 1971a, "Dynamic Analysis of Mechanical Systems with Clearances, Part 1: Formation of the Dynamic Model," *ASME Journal of Engineering for Industry*, Vol. 93, pp. 305–309.

Dubowsky, S., and Freudenstein, F., 1971b, "Dynamic Analysis of Mechanical Systems with Clearances, Part 2: Dynamic Response," *ASME Journal of Engineering for Industry*, Vol. 93, pp. 310–316.

Dutson, J. D., and Folkman, S. L., 1996, "A Nonlinear Finite Element Model of a Truss Using Pinned Joints," in *Proceedings of the 37th AIAA/ASME/ASCE/AHS/ASC Structures, Structural Dynamics and Materials Conference*, Salt Lake City, pp. 793–803.

Ferri, A. A., 1988, "Modeling and Analysis of Nonlinear Sleeve Joints of Large Space Structures," *AIAA Journal of Spacecraft and Rockets*, Vol. 25, pp. 354–365.

Folkman, S. L., Rowsell, E. A., and Ferney, G. D., 1995, "Influence of Pinned Joints on Damping and Dynamic Behavior of a Truss," *Journal of Guidance Control, and Dynamics*, Vol. 18, pp. 1398–1403.

Masri, S. F., and Caughey, T. K., 1979, "A Nonparametric Identification Technique for Nonlinear Dynamic Problems," *Journal of Applied Mechanics*, Vol. 46, pp. 433–447.

Masters, B. P., and Crawley, E. F., 1994, "Multiple Degree of Freedom Force-State Component Identification," *AIAA Journal*, Vol. 32, pp. 2276–2285.

Masters, B. P., Crawley, E. F., and van Schoor, M. C., 1996, "Global Structure Modeling Using Force-State Component Identification," *Journal of Guidance, Control, and Dynamics*, Vol. 19, pp. 198–206.